PHILOSOPHICAL TRANSACTIONS OF THE ROYAL SOCIETY A MATHEMATICAL, PHYSICAL & ENGINEERING SCIENCES

Flare Energy Transport by Conduction and Radiation [and Discussion]

Marcos E. Machado, M. G. Haines, E. R. Priest and J. C. Henoux

Phil. Trans. R. Soc. Lond. A 1991 **336**, 425-437
doi: 10.1098/rsta.1991.0092

Flare energy transport by conduction and radiation

By Marcos E. Machado

Department of Physics, The University of Alabama in Huntsville, Huntsville, Alabama 35899, U.S.A.

As energy is released in coronal flare loops, strong temperature gradients may appear and large-scale flows can be set up. In the absence of, or in addition to, energetic particle beams, thermal conduction and mass motions are major processes that distribute energy throughout the flare atmosphere. We review basic physical concepts of the energy transport processes, and their observational evidence. We then turn to radiative energy transport, an often ignored processes that may constitute a major transfer mechanism, particularly into and throughout the dense, optically thick, chromospheric and photospheric layers. The basic physics of radiative energy transport is reviewed, and some specific examples discussed in detail, particularly in connection with upper photosphere heating and white light flare events.

1. Introduction

A primary manifestation of flare activity is the generation of high-temperature (greater than 10^7 K) plasma in coronal magnetic loop structures. Other papers in this volume deal with various contentious issues regarding the role of non-thermal particles in solar flares. Instead, it can barely be disputed that the generation of a hot coronal source, by any plausible mechanism, should set up a strong temperature gradient and energy will then be transported into the undisturbed surroundings and the cool chromosphere.

Furthermore, X-ray ultraviolet (XUV) observation have also shown that the radiation of the hot plasma constitutes a major fraction of the overall flare radiative output (Canfield *et al.* 1980; Wu *et al.* 1986). It has been recognized by several authors (Somov 1975; Hénoux & Nakagawa 1977; Machado 1978) that a considerable amount of energy is transported radiatively both towards the heliosphere as well as downwards into the chromosphere and upper photosphere. Indeed, in a detailed study of a flare observed by *Skylab*, Withbroe (1978) found that its total radiative output was $E_r = 2.2 \times 10^{31}$ erg†, while thermal conduction losses from the hot coronal plasma were $E_c = 1.4 \times 10^{31}$ erg throughout the gradual phase. Because half of E_r goes downwards, these results show that radiative energy transport can be comparable with that due to conduction. This is particularly true during the gradual phase but, as we show below, radiative processes may also play an important role during the impulsive phase of energy release.

† 1 erg = 10^{-7} J.

Phil. Trans. R. Soc. Lond. A (1991) **336**, 425–437
Printed in Great Britain

Basic theoretical concepts and observations pertaining to these processes are reviewed in the remainder of this paper.

2. Heat conduction: an overview

The equation of classical heat conduction is (Spitzer 1962)

$$F_{\rm cl} = \kappa T^{\frac{5}{2}} \nabla T \,\mathrm{erg\,cm^{-2}\,s^{-1}}, \tag{1}$$

where F is the thermal flux, κ is the classical Spitzer coefficient (*ca.* 1.1×10^{-6} erg cm^{-2} s^{-1} K$^{-\frac{7}{2}}$). In flaring loops, since heat conduction across field lines is greatly suppressed, the temperature gradient can be written as $\nabla T = \mathrm{d}T/\mathrm{d}s$, where s is the coordinate along the loop (figure 1).

For 'typical' flare conditions, $T_{\rm cor} \approx 10^7$ K and $L \approx 10^9$ cm, where $T_{\rm cor}$ is the coronal temperature and L is the loop length, $\mathrm{d}T/\mathrm{d}s$ can be approximated as $2T/L$ (where we use $\frac{1}{2}L$ as the temperature variation scale length, $L_{\rm T}$), and equation (1) gives $F_{\rm cl} \approx 6 \times 10^9$ erg cm^{-2} s^{-1} as the flux conducted into the cool (less than 10^5 K) layers of atmosphere. This value is 10^3 times larger than the one obtained for quiescent loops in hydrostatic equilibrium, implying, as we shall see below, that a major dynamic rearrangement of the atmosphere should occur in response to flare heating.

Equation (1) is valid only when the temperature variation scale length is large compared with the electron mean free path ($\lambda_{\rm e}$). When $L_{\rm T}/\lambda_{\rm e} > 0.1$ it begins to overestimate the conductive fluxes (see, for example, Campbell 1983), until it eventually exceeds the saturated flux limit, given by the thermal energy density of the heated plasma multiplied by a streaming velocity, $v_{\rm s}$,

$$F_{\rm sat} = [\tfrac{3}{2} nkT]\, v_{\rm s}. \tag{2}$$

When we assume that $v_{\rm s} = v_{\rm e}$, where $v_{\rm e}$ is the electron thermal speed, we obtain an absolute limit case of uncompensated free-flight of all plasma electrons from the hot source. This is, however, an unrealistic situation, because to ensure a zero net number flux of electrons that permeate into the cooler plasma, a return-current must be set in. Manheimer & Klein (1975) have shown that an appropriate approximation to the saturated flux is given by letting $v_{\rm s} = \frac{1}{6} v_{\rm e}$ so that

$$F_{\rm sat} \approx \tfrac{1}{4} n m_{\rm e} v_{\rm e}^3 \tag{3}$$

Then, the ratio between classical and saturated fluxes is, replacing numerical constants,

$$F_{\rm cl}/F_{\rm sat} \approx 6.9 \times 10^4\, n^{-1}\, T \nabla T, \tag{4}$$

which shows that our 'typical flare loop' is within the classical régime as long as $n > 10^{10}$ cm^{-3}. This is not true, however, if just small regions within the loop are heated to very high temperature (greater than 10^8 K). In such a case, further flux limitations can occur due to collective plasma effects associated with the bulk steaming of electrons. If the electron–ion temperature ratio $T_{\rm e}/T_{\rm i} \gg 1$ in the downstream plasma, the high speed can set up ion-acoustic waves that enhance the collision frequency, effectively reducing the heat flux out of the heated region. This happens because turbulence develops at the boundaries of the hot plasma, which then becomes bounded by relatively thin conduction fronts that propagate along field lines. At the limit, F becomes the anomalous heat flux, given by

$$F_{\rm an} = \tfrac{3}{2} nkT_{\rm e}\, c_{\rm s}, \tag{5}$$

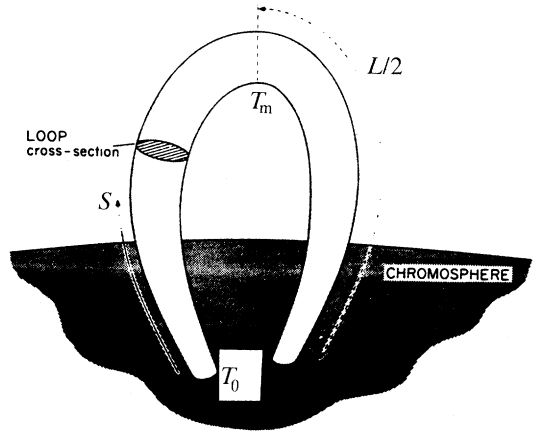

Figure 1. Schematic representation of a single flaring loop (after Withbroe 1981).

where c_s is the ion sound speed. Smith & Lilliequist (1977; see also Tandberg-Hanssen & Emslie 1988) give appropriate expressions to calculate F_{an} for different values of T_e/T_i.

The concept of anomalous flux limitations has been incorporated in the development of the 'dissipative thermal model' of hard X-ray bursts (Brown *et al.* 1979; Smith & Lilliequist 1979; see Vlahos *et al.* 1986; Dennis & Schwartz 1989 for reviews). In such a model, impulsively heated plasma is confined by the conduction fronts, reducing its cooling and implying that a substantial fraction of observed 10–10^3 eV emission is due to thermal bremsstrahlung by the bottled-up electrons. The hot (10^8 K) electrons interact among themselves and do not experience the major collision losses of thick-target model beam electrons with cool chromospheric electrons, which are the main cause of their low (10^{-5} of total beam energy) radiation efficiency.

An important property of the anomalous conduction fronts is that they are leaky and self-regulating (Heyvaerts 1981). High-energy electrons in the tail of the distribution can escape, because as in any ordinary plasma the collision cross section at the front scales as v^{-1}, and the escape speed is

$$v_{esc} = v_e(m_i/m_e)^{\frac{1}{6}} \approx 3\,v_e. \tag{6}$$

This implies that thermal tail electrons will stream freely and emit hard X-rays in a thick-target pulse fashion at the footpoints of the loop. Therefore, a continuous burst of high-energy X-rays demands that the tail must be somehow regenerated. On the other hand, the process is self-regulating because the leakage adapts so as to allow the escape of fast electrons with such a flux that gives rise to the maximum return current in the downstream plasma.

3. Heat conduction: observations

(*a*) *Static models*

When continuous heating occurs over timescales longer than the hydrodynamic response timescale of flaring loop ($\tau_h \approx L/c_s$) pressure equilibration is attained and relatively simple models can be used to interpret XUV flare observations. Shmeleva

& Syrovatskii (1973, hereafter referred to as SS) developed an elegant model to compute the temperature and emission measure distribution in a stationary heated atmosphere. They assumed that at all atmosphere levels there is a balance between conductive heating (classical) and radiative cooling, so that

$$\frac{\mathrm{d}}{\mathrm{d}s}\left(\kappa T^{\frac{5}{2}}\frac{\mathrm{d}T}{\mathrm{d}s}\right)+P_{\mathrm{I}}=n^2\Phi(T), \tag{7}$$

where $\Phi(T)$ is the optically thin radiative loss function (Cox & Tucker 1969; Raymond *et al.* 1976), and P_{I} is a (fixed) heating parameter of the form $P_{\mathrm{I}}\approx n^{\alpha}$ which, under the assumption of uniform pressure, becomes proportional to $T^{-\alpha}$, since

$$n(s)\,T(s)=n_0\,T_0=\text{const.}, \tag{8}$$

where n_0 and T_0 are the density and temperature at a, somewhat arbitrary, chromospheric boundary. They were then able to represent the heat flux in the form

$$F(T)=f(T)\,F_0, \tag{9}$$

where $f(T)$ is a dimensionless function and F_0 is the unit energy flux, which depends on n_0. Besides the uniform pressure case, SS also obtained a solution for the limiting case of impulsive heating, where they did not allow the preflare density structure to change.

Machado & Emslie (1979) revised the SS models, introducing a loop geometry with a temperature maximum at its apex, where $\nabla T=0$ as well as its chromospheric boundary, and also let $\nabla\cdot F\neq 0$ at the chromosphere, whereas SS had assumed $\nabla\cdot F=\nabla T=0$ at the lower boundary. They also obtained an $f(T)$ function similar to that of SS and calculated the distribution of the differential emission measure as a function of temperature defined as (Withbroe 1975)

$$Q(T)\,\mathrm{d}T=n_e^2\,\mathrm{d}s, \tag{10}$$

which can be written in the form

$$Q(T)\,\nabla T=(p/kT)^2, \tag{11}$$

where p is the gas pressure and then

$$F_{\mathrm{cl}}=kT^{\frac{5}{2}}\nabla T=k(p/k)^2T^{\frac{1}{2}}/Q(T). \tag{12}$$

For a given $Q(T)$, the intensity of a spectral line is (see Withbroe 1975)

$$I_\lambda=1.75\times10^{-16}\,Af\int gG(T)\,Q(T)\,\mathrm{d}T, \tag{13}$$

so that from observation of spectral lines at different temperatures $Q(T)$ can be calculated iteratively, as discussed by Withbroe.

Skylab extreme ultraviolet (EUV) observations were used by Machado & Emslie (1979) as well as several other authors (see, for example, Canfield *et al.* 1980; Craig 1981) to derive $Q(T)$ distribution of flares. It is interesting to note that implicit in the SS-type model, where pressure is uniform and optically thin radiative losses balance conductive heating, there is a one to one correlation between $Q(T)$, pressure and conductive flux. This has been demonstrated to hold in hydrodynamic calculations by Fisher *et al.* (1985), but overlooked by Richiazzi & Canfield (1980), who varied p and F arbitrarily in their static model calculations.

The overall result of *Skylab* data analyses was that, to a first-order approximation, observed EUV and XUV line intensities led to $Q(T)$ distributions in accordance with the SS-type model predictions, with

$$5\times10^{16} \lesssim nT \lesssim 3\times10^{18}\ \mathrm{cm^{-3}\ K} \tag{14}$$

in various types of events, and estimated conductive fluxes at the 10^5 K level, F_{c5}

$$5\times10^{6} \lesssim F_{c} \lesssim 10^{8}\ \mathrm{erg\ cm^{-2}\ s^{-1}}. \tag{15}$$

These numbers, for individual events, are comparable with observed Lyman-α (Lα) fluxes, suggesting a causal relation when we note that Lα is the major radiative loss agent at $T < 10^5$ K. Also, from the pressures obtained, noticing that there is a little mass between the transition zone and the base of the loop, we can obtain the mass column density at the top of the chromosphere using the hydrostatic relation

$$m_0 = (n_0\, T_0\, k/g_0)\ \mathrm{g\ cm^{-2}}, \tag{16}$$

which gives,

$$1.5\times10^{-4} \leqslant m_0 \leqslant 8\times10^{-3}\ \mathrm{g\ cm^{-2}} \tag{17}$$

for the nT values quoted above. These numbers can be compared with the quiet Sun value, $m_0(\mathrm{QS}) \approx 8\times10^{-6}$ g cm^{-2}, to give $\Delta m = m_0(\mathrm{flare}) - m_0(\mathrm{QS})$ as the amount of material heated to coronal flare temperatures.

(*b*) *Dynamic models*

Many authors (see, for example, Pallavicini *et al.* 1983; MacNeice *et al.* 1984; Emslie & Nagai 1985; Fisher *et al.* 1985; see recent reviews by Antonucci 1989; Peres 1989) have computed models that describe the evolution of a flaring loop in response to localized heating, generally assumed to be at the top of the loop.

The basic physical concepts, regarding the expected response of a loop to such an input, are given in a review by Craig (1981). By increasing the apex temperature, propagating thermal fronts are created and mass motions set-in due to pressure imbalance. Upon reaching the chromosphere–corona transition region, the fronts overheat the radiatively unstable plasma at temperatures less than 10^5 K causing a localized pressure enhancement that leads to an upwards convective flow of X-ray emitting plasma, the 'chromospheric evaporation' process. This sequence of phenomena is depicted in figure 2, where we have taken, as a representative example, the calculations of Emslie & Nagai (1985). Eventually, if heating continues long enough, the atmosphere adjusts to a steady-state situation as described in §3*a*.

A notable feature of the hydrodynamic calculations is the downward propagation of cold plasma, i.e. a 'chromospheric condensation', whose properties have been studied in detail by Fisher (1989). These condensations are most notable in particle heated flare models, but occur in all conditions and their duration is rather insensitive to the details of flare heating.

Observational evidence of chromospheric evaporation is given by blue-shifted soft X-ray line profiles and hydrogen Hα profiles that show a red asymmetry (Zarro *et al.* 1988). The details of these studies are described elsewhere in this volume.

On the other hand 3.5 keV (or greater) images recorded by *SMM*s hard X-ray imaging spectrometer (HXIS) (van Beek *et al.* 1980) have been used to infer the existence and propagation of thermal fronts. The spatial resolution of these data was too low to detect motions in structures comparable with our 'typical' flare loop, but sufficient to see X-ray fronts propagate along large scale (10^5 km) magnetic loops. Rust *et al.* (1985), found seven cases in which this type of phenomenon could

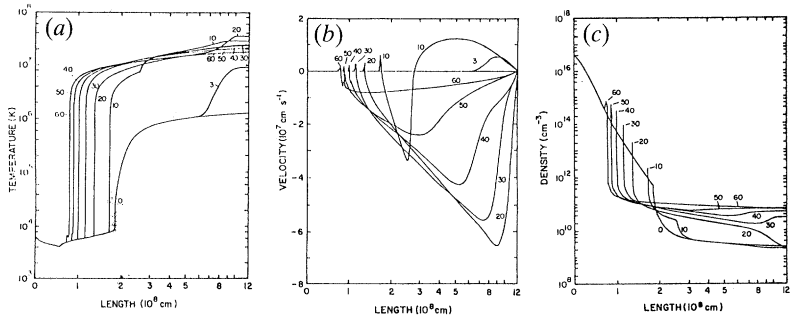

Figure 2. Time development of (*a*) temperature, (*b*) macroscopic velocity and (*c*) density as a function of position in Emslie & Nagai's hydrodynamic flare loop models. Only half loop is shown, because of symmetry. Curve labels signal the time elapsed (in seconds) after the start of the heating. Negative velocities are directed upwards. Note that at 3 s the coronal material moves downwards, due to the initial heating at the top of the loop, while at later times the motion is primarily upwards, signalling the effect of chromospheric evaporation. Also note that a high density 'chromospheric condensation' develops at the bottom of the flare transition zone and moves downwards.

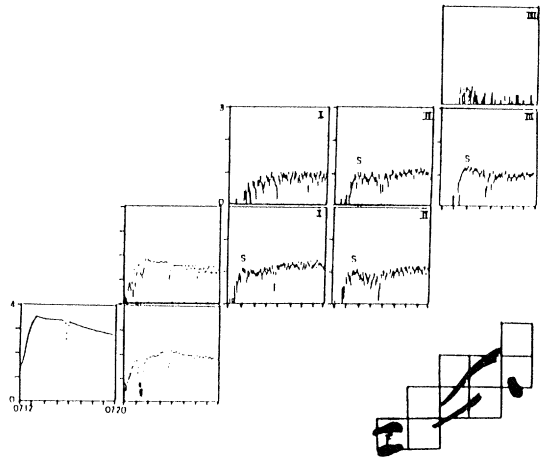

Figure 3. Set of 3.5–8.0 keV individual pixels (32 arcsec in resolution) lightcurves (log counts per second), of a flare (pixel labelled F) and large-scale loops observed by HXIS on 9 May 1980. Note the propagation of 'hump' S through regions I, II and II, which cover the large loops depicted in the insert. Data dropouts in the two pixels closest to the flare site are of instrumental origin (see Machado *et al.* 1988).

be observed, where they could estimate propagation speeds ranging from 800–1700 km s^{-1}. In three cases where Hα images were available, they showed brightenings at the feet of the large-scale loops when the moving fronts arrived. These properties are consistent with predictions of conductively heated flare loop models. They inferred non-classical heat fluxes of up to 10^{10} erg cm^{-2} s^{-1}.

The events studied by Rust *et al.* (1985) were too weak, in X-rays, to allow them to determine parameters such as temperature and emission measure at the X-ray fronts. Instead, Machado *et al.* (1988) studied the brightest event recorded by HXIS where count rates were large enough to obtain physical parameters from observed band ratios. The characteristics of the event are depicted in figures 3 and 4. The large-scale structure seen in figure 3 is a system of long loops (greater than 87 000 km)

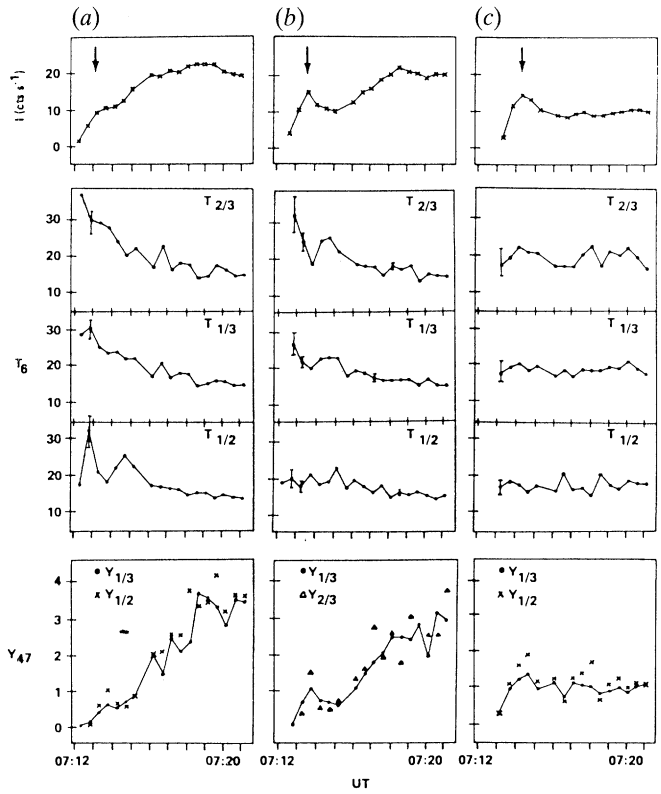

Figure 4. Intensity, temperature (in 10^6 K) and emission measure labelled Y (in 10^{47} cm^{-3}), for the three large-loop regions ((*a*) I, (*b*) II, (*c*) III) shown in figure 3. The different temperature estimates are from HXIS band ratios band 2/band 3 (5.5–8.0 keV/8.0–11.5 keV), band 1/band 3 (3.5–5.5 keV/8.0–11.5 keV) and band 1/band 2, as labelled. Emission measure values are obtained from temperature estimates and absolute counting rates in the bands. Note that the intensity hump is related to an increase in emission measure, which is preceded by a high temperature front and followed by a slow and steady rise in *Y*. The arrows show the time of the hump in each region.

through which a moving 3.5–8.0 keV 'hump', S, propagated at a speed $\geqslant 900$ km s^{-1}. As seen in the light curves, this front is followed by a slower and gradual increase in X-ray intensity, which moves at a slower speed of *ca.* 200 km s^{-1}. From the temperature and emission measure analysis, shown in figure 4, we see that S is associated with a propagating increase in emission measure, $Y \approx 10^{47}$ cm^{-3}. This hump is, however, preceded by a high-temperature front, with T values showing a decreasing trend through its propagation along the structure. The slower and gradual enhancement in X-ray emission is due to steady increase in emission measure over a period of minutes. Finally, Hα observations showed impulsive brightenings at the far end footpoints early during the impulsive phase of the flare, and a stronger and more steady brightening at the arrival of the front.

These results are consistent with the conclusions of Craig & McClymont (1976; see also Craig 1981; Craig & Davys 1984) on the effects associated with bulk heating of coronal flare plasma. As shown in figure 5 the high-temperature front can be interpreted as a conduction front which is followed by a shock wave and compressed plasma (the hump, S), whose X-ray increase is due to slower evaporation of material from the primary footpoint. Machado *et al.* (1988) also note the consistency of these

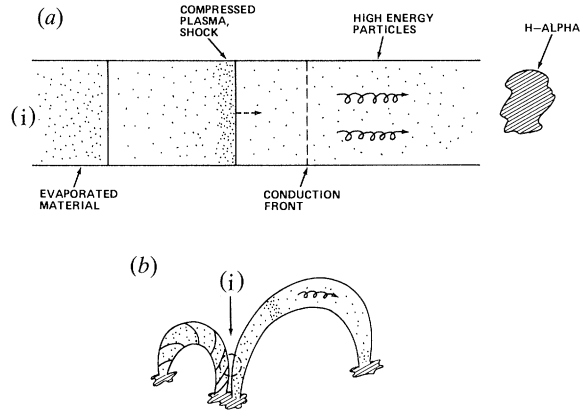

Figure 5. Schematic representation (*a*) of phenomena observed during the 9 May event. Independent evidence (not discussed here) shows that accelerated particles were injected into the large loop(s), and were followed by a conduction front, a shock that slowly overtakes it, and material evaporated from the primary footpoint. The event is interpreted (*b*) as comprising a highly sheared flare loop (F site in figure 3) and a large-scale loop or loop system that interacts with it at some interface (i).

observational results with the predictions of the self-similar analysis of Zeldovich & Raizer (1967) in the limit of impulsive, localized heating.

By using an estimate of the density, $n \approx 4 \times 10^9$ cm^{-3}, derived from X-ray and UV observations, and a front speed $v_f = 10^8$ cm s^{-1}, we obtain

$$F_c \approx 1.5\, n m_e v_e^2 v_f \approx 4.3 \times 10^9 \text{ erg cm}^{-2} \text{ s}^{-1}, \tag{18}$$

which lies between saturated, $F_{sat} \approx 7 \times 10^9$ erg cm^{-2} s^{-1}, and anomalous, $F_{an} \approx 10^9$ erg cm^{-2} s^{-1} limits (cf. equations (3) and (5)). The results are thus consistent with flux limitation, as expected, but do not give evidence of anomalous flux processes.

4. Radiative energy transport: an overview

As noted in §1 a substantial amount of energy is transported radiatively from the coronal loops towards the deep atmosphere layers. Somov (1975) was the first to recognize it and suggest that, at least part of, the chromospheric flare heating was due to XUV irradiation. Hénoux & Nakagawa (1977) were the first to study the effect of chromospheric soft X-ray irradiation in detail. Also, Somov & Syrovatskii (1976) and Machado & Hénoux (1982), investigated the effects of UV radiation.

The basic physical processes that describe the interaction between XUV photons and ambient chromospheric plasma were discussed in detail by Hénoux & Nakagawa (1977). The incoming photons are energetic enough to over ionize some of the abundant chromospheric species such as H, He, C, N, O and Si, changing their ionization balance, schematically given by

$$n^+/n^0 = (P + C)/R, \tag{19}$$

where P, C and R are the photoionization, collisional ionization and recombination rates respectively. For a species A, P is given by

$$P^A = 4\pi \int (\sigma_\lambda^A J_\lambda / h\nu)\, d\lambda, \tag{20}$$

where σ_λ^A is the photoionization cross section and J_λ is the radiation field mean

intensity 'seen' by the atom. A flare associated increase in J_λ causes the n^+/n^0 ratio to increase by direct photoionization, and creates suprathermal 'photoelectrons' which interact with ambient particles (primarily thermal electrons), leading to net atmospheric heating. As in any chromospheric flare heating calculation, the radiative heating is balanced by an increase in lines and continua radiative losses.

Hénoux & Nakagawa (1977) and Fang & Hénoux (1983) computed the distribution of energy input as a function of chromospheric mass column density, $m-m_0$ (g cm^{-2}), where m_0 is the column mass at the top of the chromosphere. By using a medium intensity X-ray flare flux, they found that the energy input rate matched the energy loss rates of semi-empirical models of the chromosphere (see, for example, Machado *et al.* 1980; Avrett *et al.* 1986), based on observed flare spectra. This shows, in quantitative terms, what our previous order of magnitude estimates had suggested, i.e. that soft X-ray heating can account for the flare chromospheric temperature enhancements.

Somov & Syrovatskii (1976) also suggested that EUV radiation (1000–1600 Å†), originating mainly in the conductively heated flare transition zone, could provide an additional energy input to low chromospheric flare regions, comparable to that of soft X-ray irradiation. This possibility was studied in detail by Machado & Hénoux (1982) who demonstrated that, contrary to Somov & Syrovatskii's expectations, EUV and UV line radiation just constitute a minor contribution to the energy input by radiation.

On the other hand, Machado & Hénoux (1982) showed that, despite their insignificant heating role, transition zone line radiation may have a strong effect in the ionization balance of elements like C$^{\mathrm{I}}$ (in the upper chromosphere) and Si$^{\mathrm{I}}$ (at the temperature minimum region, TMR). The most notable effect is on silicon atoms, because due to the low temperatures of the TMR and consequently low electron densities in the region, a change in the photoionization rate has a much stronger effect than any plausible increase in collisional ionization (cf. equation (19)). Machado & Hénoux showed that Si$^{\mathrm{I}}$ photoionization rates can increase by a factor of 10 at the TMR, due to irradiation by UV line emission, particularly the C$^{\mathrm{IV}}$ line at 1545 Å.

An increase in the Si$^{\mathrm{II}}$/Si$^{\mathrm{I}}$ ratio, induced by larger photoionization, has two seemingly opposite diagnostic effects which serve as an ideal example to show the complex interplay of radiative energy transport and ionization processes. First of all, since the silicon ionization balance is governed by non-local radiative sources, its ^{3}P and ^{1}D continua (with edges at 1525 Å and 1682 Å respectively) have source functions that are strongly decoupled from ambient temperature conditions. In fact, since the radiation field 'seen' by the atoms is much larger than the one produced locally, the source function of both continua become much larger than the local Planck function at the same wavelength, $S_\lambda > B_\lambda(T)$. As shown by Machado & Hénoux (1982), this results in a substantial increase in the continuum brightness temperature, $T_\mathrm{b} \approx 4700$ K as compared with the quiet Sun value $T_\mathrm{b} \approx 4450$ K, without any ambient temperature increase. Therefore, it is clearly erroneous to infer temperature enhancements from an increase in the silicon continua brightness temperature.

On the other hand, the missing part of the story is that the temperature is really enhanced at the TMR during flares (see, for example, Machado *et al.* 1978; Cook 1979).

† 1 Å = 10^{-10} m = 10^{-1} nm.

PHILOSOPHICAL TRANSACTIONS OF THE ROYAL SOCIETY A MATHEMATICAL, PHYSICAL & ENGINEERING SCIENCES

Machado *et al.* (1978) argued that canonical energy transport processes (heat conduction, accelerated particles and soft X-rays) are too strongly attenuated in the chromosphere and cannot account for the required heating rate. Abondarham & Hénoux (1989) have refined this type of calculations and shown that, under some circumstances, the required TMR heating can be effected by beams of electrons accelerated during the impulsive phase of the flare. Still, the problem is that TMR heating is not just an impulsive phenomena.

Machado *et al.* (1986) re-examined the role of the negative hydrogen ion, H^-, at the TMR. They found that, in contrast with assumptions by earlier authors (notably Machado *et al.* 1978, and subsequent papers based on their simplified approach), H^- is a source of heating at these levels (a well known quiet Sun property). Furthermore, they found that the excess ionization of silicon, as discussed above, causes a considerable increase in the TMR electron number density, since most species are largely neutral at those levels. This in turn increases the electron–neutral-hydrogen association rate and, thus, the H^- abundance. Then, since the negative hydrogen ion is the main absorber of photospheric radiation, this chain of processes leads to an increase in its absorption and increased heating, by radiant energy coming from below at the quiet Sun rate. Then, by this process, the observed TMR flare temperature (*ca.* 4800 K) is obtained through minimal energy transport by canonical processes, and can be sustained for as long as ionizing radiation fluxes are large enough to maintain an increased Si^{II}/Si^{I} ratio.

5. Radiative energy transport: observations

As already noted in the previous section, observational tests of the soft X-ray mechanism are almost always based on the comparison between theoretical and semi-empirical models. Except for one exception (Gan & Fang 1990), calculations to date show that X-ray heating rates are large enough to produce the required chromospheric temperature enhancements (Hénoux & Nakagawa 1977; Machado 1978; Hénoux & Rust 1980; Fang & Hénoux 1983; Machado *et al.* 1989). It is, however, desirable to have model independent evidence. Searching for such an evidence, Machado (1978) studied Lα and Lyman continuum images of a compact and a two ribbon flare. He found haloes around the compact X-ray source as well as around the bright flare ribbons (where Lyman radiation is largely due to heat conduction), in agreement with predictions of the irradiation model. These results, however, have not had independent confirmation, mainly because of lack of appropriate datasets. On the other hand, it has been suggested by Machado (1982) that temporal differences, observed in light curves of lines formed at different chromospheric levels (Lemaire *et al.* 1982), are consistent with a picture in which lines formed at the top of the chromosphere respond to heat conduction, and lines formed deeper to soft X-ray heating.

Theoretical predictions of the UV irradiation were tested, among other possibilities, by Metcalf *et al.* (1990). By using two Mg^{I} lines, as indicators of temperature and electron density variations at the TMR, they studied the temporal evolution of these parameters in five solar flares. They find that the extended heating observed in two flares can be explained by UV irradiation. On the other hand, the initial effects observed in all five events are consistent with backwarming by enhanced upper chromosphere Balmer and Paschen continuum radiation, as proposed by Aboudarham & Hénoux (1987). In all cases, they were able to eliminate non-

PHILOSOPHICAL TRANSACTIONS OF THE ROYAL SOCIETY A MATHEMATICAL, PHYSICAL & ENGINEERING SCIENCES

radiative effects such as heating by currents (Emslie & Machado 1979), electron and proton beams (as expected) soft X-rays (as expected), and dissipation of Alfvén waves (Emslie & Sturrock 1982).

6. The future

In the previous sections we have concentrated on the basic physics of energy transport by conduction and radiation, as well as on past work about their observational evidence. We may now ask ourselves what new developments we foresee in the near future. To do so, we shall change the order of the approach used throughout the paper and start with observations.

Among many projects it is quite obvious that the *Solar-A* mission, described elsewhere in this volume, will play a major role in the research to come. Its payload, particularly the soft X-ray telescope, Bragg spectrometer and hard X-ray imager, will give new information on the role of soft X-ray emission, dynamics of high-temperature plasma regions, and the role of conduction fronts and shocks as compared with that of energetic particles. *Skylab* gave us excellent X-ray pictures and line spectroscopy, with poor temporal resolution and no information on high-energy phenomena. The *SMM* gave us good time resolution, hard X-ray imaging and good X-ray spectra, but lacked the high spatial resolution of *Skylab* (except in its UV telescope). *Solar-A* will provide an excellent combination of most of the major features of these two missions, with further improved sensitivity. It will lack, however, the capability of transition region diagnostics which, as we have seen, was extremely useful in the early analyses from *Skylab*. It is something to be kept in mind for future missions. Ground-based telescopes and balloon experiments will also contribute greatly to our understanding of flare phenomena. It is clear (see Canfield *et al.* 1991) that vector field measurements combined with spacecraft and ground-based data can, eventually, shed light into the understanding of the complex interplay of transport processes and their relation to the magnetic field configuration. The same occurs with high spectral resolution hard X-ray balloon observations, as discussed by Brown (1991).

On the theoretical side, work is required on the effects of non-maxwellian distribution functions in flaring loops and the chromosphere-transition region (see, for example, Ljepojevic & MacNeice 1988; MacNeice *et al.* 1991), to understand its physical and observational consequences and signatures. The role of conductive flux limitation, as discussed above, has been dealt with in an as yet rather schematic and *ad hoc* way. It certainly deserves a more rigorous treatment because of its profound implications about the overall energy budget. Finally, the possibly major role of radiation as an energy transport process in the chromosphere and photosphere, is a topic to be addressed in detail and in combination with other transport processes, like particle beams and heat conduction. As an example, we cite again the results of Aboudarham & Hénoux (1987) and Metcalf *et al.* (1990), on the possible role of hydrogen continuum photons as the cause of TMR temperature enhancements and white light flares. Similarly, Machado *et al.* (1989) have also speculated on the role of soft X-ray heating and Balmer continuum emitting chromospheric condensations, as a way to radiatively transport energy from the flare chromosphere to the photosphere, where visible continuum radiation originates.

The author thanks the Royal Society for providing the financial support that allowed him to attend the Discussion Meeting. This work has been sponsored by NASA Grants NAG8-817 and NAG8-843.

PHILOSOPHICAL TRANSACTIONS OF THE ROYAL SOCIETY A MATHEMATICAL, PHYSICAL & ENGINEERING SCIENCES

References

Aboudarham, J. & Hénoux, J. C. 1987 *Astron. Astrophys.* **174**, 270.

Antonucci, E. 1989 *Solar Phys.* **121**, 31.

Avrett, E. H., Machado, M. E. & Kurucz, R. 1986 In *The lower atmosphere of solar flares* (ed. D. F. Neidig), p. 246. New Mexico: Sunspot.

Brown, J. C. 1991 *Phil. Trans. R. Soc. Lond.* A **336**, 413–424. (This volume.)

Brown, J. C., Melrose, D. B. & Spicer, D. S. 1979 *Astrophys. J.* **228**, 592.

Campbell, P. M. 1984 *Phys. Rev.* A **30**, 365.

Canfield, R. C. *et al.* 1980 In *Solar flares, a monograph from Skylab workshop II* (ed. P. A. Sturrock), p. 451. Colorado University Press.

Canfield, R. C., de La Beaujardiere, J. & Leka, K. D. 1991 *Phil. Trans. R. Soc. Lond.* A **336**, 381–388. (This volume.)

Cook, J. 1979 *Astrophys. J.* **234**, 378.

Cox, D. P. & Tucker, W. H. 1969 *Astrophys. J.* **157**, 1157.

Craig, I. 1981 In *Solar flare magnetohydrodynamics* (ed. E. Priest), p. 277. Gordon and Breach.

Craig, I. & McClymont, A. N. 1976 *Solar Phys.* **50**, 133.

Craig, I. & Davys, J. W. 1984 *Solar Phys.* **90**, 343.

Dennis, B. R. & Schwarts, R. 1989 *Solar Phys.* **121**, 75.

Emslie, A. G. & Machado, M. E. 1979 *Solar Phys.* **64**, 129.

Emslie, A. G. & Nagai, F. 1985 *Astrophys. J.* **288**, 779.

Emslie, A. G. & Sturrock, P. A. 1982 *Solar Phys.* **80**, 99.

Fang, C. & Hénoux, J. C. 1983 *Astron. Astrophys.* **118**, 139.

Fisher, G. H. 1989 *Astrophys. J.* **346**, 1019.

Fisher, G. H., Canfield, R. C. & McClymont, A. N. 1985 *Astrophys. J.* **289**, 425.

Gan, W. Q. & Fang, C. 1990 *Astrophys. J.* **358**, 328.

Hénoux, J. C. & Nakagawa, Y. 1977 *Astron. Astrophys.* **57**, 105.

Hénoux, J. C. & Rust, D. M. 1980 *Astron. Astrophys.* **91**, 322.

Heyvaerts, J. 1981 In *Solar flare magnetohydrodynamics* (ed. E. Priest), p. 429. Gordon and Breach.

Lemaire, P., Choucq-Bruston, M. & Vial, J. C. 1982 *Solar Phys.* **90**, 63.

Ljepojevic, N. N. & MacNeice, P. 1988 *Solar Phys.* **117**, 123.

Machado, M. E. 1978 *Solar Phys.* **42**, 235.

Machado, M. E. 1982 *Adv. Space Res.* **2**, 115.

Machado, M. E., Emslie, A. G. & Brown, J. C. 1978 *Solar Phys.* **58**, 363.

Machado, M. E. & Emslie, A. G. 1979 *Astrophys. J.* **232**, 903.

Machado, M. E., Avrett, E. H., Vernazza, J. E. & Noyes, R. W. 1980 *Astrophys. J.* **242**, 336.

Machado, M. E. & Hénoux, J. C. 1982 *Astron. Astrophys.* **108**, 61.

Machado, M. E., Emslie, A. G. & Mauas, P. J. D. 1986 *Astron. Astrophys.* **159**, 33.

Machado, M. E., Xiao, Y. C., Wu, S. T., Prokakis, Th. & Dialetis, D. 1988 *Astrophys. J.* **326**, 451.

Machado, M. E., Emslie, A. G. & Avrett, E. H. 1989 *Solar Phys.* **124**, 303.

MacNeice, P., McWhiter, P., Spicer, D. S. & Burgess, A. 1984 *Solar Phys.* **90**, 357.

MacNeice, P., Fontenla, J. & Ljepojevic, N. N. 1991 *Astrophys. J.* **369**, 544.

Manheimer, W. H. & Klein, H. H. 1975 *Phys. Fluids* **18**, 1299.

Metcalf, T., Canfield, R. C. & Saba, J. 1990 *Astrophys. J.* **365**, 391.

Pallavicini, R. *et al.* 1983 *Astrophys. J.* **270**, 270.

Peres, G. 1989 *Solar Phys.* **121**, 289.

Richiazzi, P. & Canfield, R. C. 1983 *Astrophys. J.* **272**, 739.

Rust, D. M., Simnett, G. M. & Smith, D. F. 1985 *Astrophys. J.* **288**, 401.

Shmeleva, O. B. & Syrovatskii, S. I. 1973 *Solar Phys.* **33**, 341.

Smith, D. F. & Lilliequist, C. G. 1979 *Astrophys. J.* **232**, 582.

PHILOSOPHICAL TRANSACTIONS OF THE ROYAL SOCIETY A MATHEMATICAL, PHYSICAL & ENGINEERING SCIENCES

Somov, B. V. & Syrovatskii, S. I. 1976 *Soviet Phys. Usp.* **19**, 813.

Spitzer, L. 1962 *Physics of fully ionized gases*, 2nd edn. Interscience.

Tandberg-Hanssen, E. & Emslie, A. G. 1988 *The physics of solar flares*. Cambridge University Press.

van Beek, H. F., Hoyng, P., LaFleur, H. & Sinett, G. M. 1980 *Solar Phys.* **65**, 39.

Vlahos, L. *et al.* 1986 In *energetic Phenomena on the Sun* (ed. M. Kundu & B. Woodgate), p. 2-1. NASA CP-2439.

Withbroe, G. L. 1975 *Solar Phys.* **45**, 301.

Withbroe, G. L. 1978 *Astrophys. J.* **225**, 641.

Zarro, D., Canfield, R. C., Strong, K. T. & Metcalf, T. 1988 *Astrophys. J.* **324**, 582.

Zeldovich, Y. B. & Raizer, Y. P. 1967 *Physics of shock waves and high temperature hydrodynamic phenomena*. Academic Press.

Discussion

M. G. Haines (*Imperial College, U.K.*). I suggest that an improved nonlinear Fokker–Planck heat flow model be used, which should include the nature of the source of heat (e.g. inverse bremsstrahlung in laser fusion has a tendency to create a non-maxwellian electron distribution); the self-consistent electric field and modified Rosenbluth potentials are important features. The higher energy electrons have a much longer mean free path and this hot tail can give the impression of a faster moving heat front.

M. E. Machado. I agree, and I mention some papers that address this issue in the text. On the other hand, because there is no universally accepted flare theory, I find it quite difficult to see how a fully self-consistent model can be built. But your point is well taken, as something to be kept in mind by theoreticians as well as those that try to interpret observations.

E. R. Priest (*The University, St Andrews, U.K.*). The numerical simulations you mentioned assume the presence of rigid magnetic tubes and describe the hydrodynamic response to energy deposition. Such an input of energy will in practice, however, produce MHD shocks and waves, and so in future I would like to see a new generation of models which couple the MHD and energetics. A small beginning has been made by Forbes *et al.* (*Solar Phys.* **120**, 285 (1989)) but much remains to be done.

M. E. Machado. Good point. You and Professor Haines are simply showing us where we should concentrate our efforts in the future. In my paper, on the other hand, except for some speculation at the end, I was trying to give an outline of what I think are the most solid foundations of our understanding to date.

J. C. Hénoux (*Observatoire de Paris, France*). The Paschen continuum can also contribute to the backwarming of the temperature minimum region and upper photosphere. It has been shown that a significant amount of Paschen recombination emission is produced when an electron beam is bombarding the atmosphere. A simultaneous enhancement of the H^- absorption, by a mechanism you yourself pointed out, increases the efficiency of the radiative heating. As a result a white light flare is produced that includes both the contribution of the chromospheric emission and of the backwarmed upper photosphere.

PHILOSOPHICAL TRANSACTIONS OF THE ROYAL SOCIETY A MATHEMATICAL, PHYSICAL & ENGINEERING SCIENCES